Crystals of a thymidylate synthase mutant offer insights into crystal packing and plasticity of protein–protein contacts

B. Gopal*, V. Prasanna*,†, S. Parthasarathy*, D. V. Santi‡, P. Balaram*,† and M. R. N. Murthy*,§

*Molecular Biophysics Unit, Indian Institute of Science, Bangalore 560 012, India
†Chemical Biology Unit, Jawaharlal Nehru Center for Advanced Scientific Research, Bangalore 560 012, India
‡Department of Biochemistry and Molecular Biophysics, University of California, San Francisco 94143-0446, USA

Some crystal forms of thymidylate synthase from *L. casei* exhibit unit cell transformation upon irradiation by X-rays. These forms, all of which occur in the space group $P6_122$, show an elongation in the *c* cell dimension and in some cases stabilize to a constant cell dimension upon prolonged exposure. We present here an analysis of the possible causes of this transformation based on the crystal structures for two forms of an R178F mutant of this enzyme. We compare these structures to other structures with intermediate cell parameters reported in the literature. There are no large changes in the dimeric structure of TS in these crystal forms. Although there is a large change in the unit cell volume, the molecular contacts in the crystal structures are nearly invariant. The transformation appears to result from concerted small changes in molecular structure and intermolecular contacts. These observations corroborate the general impression that protein structures can accommodate minor changes in sequence or packing wherein the intra and intermolecular interactions are not seriously altered.

PROTEINS carrying out similar functions in different organisms usually have similar amino acid sequences and three-dimensional structures. The three-dimensional structure is extremely important for the function of the protein. Therefore, when amino acid replacements occur during the process of evolution, the corresponding protein structure should not undergo drastic changes, particularly so in the regions important for protein function. Structural studies have provided important clues as to how proteins adapt to mutations. For example, the deletion of a bulky side chain from the interior of a protein causes movements of the side groups and the main chain so as to compensate for the loss of stability arising due to the cavity[1].

L. casei TS is a homodimeric enzyme of molecular weight 68 kDa, and 316 residues per subunit. It catalyses the reductive methylation of deoxyuridine monophosphate with methylene tetrahydrofolate as the cofactor to produce deoxythymidine monophosphate and dihydrofolate[2]. Crystal structures have been determined for the enzyme in the presence of phosphate and deoxyuridine monophosphate[3,4]. This enzyme has been studied in our laboratory as a model system to elucidate the mechanisms of stability and folding in multimeric enzymes[5]. Mutants of TS, in which the arginine (Arg) residues occurring in the interface were replaced by other residues, were produced with a view of elucidating the role of positively charged Arg residues at the dimeric interface. One of the mutants in which an Arg was replaced by a phenylalanine (R178F mutant) was found to be 5°C more stable than the wild type TS[6].

The R178F mutant was crystallized in two different forms. The structures of these forms were determined by single crystal X-ray diffraction studies. It was also observed that one of the forms usually transforms to the other upon irradiation. It was found that the dimeric structure of TS is nearly invariant in these crystal forms and is similar to those observed in the other crystal structures of wild-type and mutant TS.

One of the major problems of structure determination by X-ray diffraction is that of radiation damage to crystals during the course of data collection. Earlier reports[7] have noted that protein crystals are particularly sensitive, probably because the lattice contacts are relatively weak and easily disrupted by radiolytic products resulting from absorbed photons. It has been suggested that at least two components contribute to the radiation damage. Primary damage is caused by energetic electrons resulting from the photoelectric, Auger or Compton effects. Secondary damage is caused by the resulting radiolytic products. These propagate through the crystal and cause further reactions and damage to the lattice contacts. These secondary processes are believed to vary greatly between different proteins and even between different crystal forms of the same protein based on the radiation sensitivity of different crystal forms. In addition to direct radiolytic processes involving X-rays, protein crystals may also be sensitive to small changes in

§For correspondence. (e-mail: mrn@mbu.iisc.ernet.in)

temperature and relative humidity during the course of data collection. The crystal structures of the R178F mutant of TS presented here illustrate that the change in unit cell volume that occurs when one form of the mutant crystal transforms to the other is not accompanied by large changes in molecular structure or contacts. It appears to result from a large number of small, concerted changes.

Materials and methods

Crystals of the R178F mutant of *L. casei* TS were obtained using the hanging drop method. The reservoir solution contained 50 mM potassium phosphate buffer pH 5.8–6.2. A 6 µl drop containing 13–15 mM ammonium sulphate in 50 mM potassium phosphate buffer pH 5.8–6.2 and 10 mg/ml protein in a hanging drop placed on a presiliconized cover-slip was equilibrated with the reservoir solution. Both forms of the crystals grew over a period of three days to sizes of $0.6 \times 0.3 \times 0.2$ mm. The crystals belong to the hexagonal space group $P6_122$, with $a = b = 79.18$ Å, $c = 244.80$ Å or $a = b = 79.30$ Å, $c = 230.89$ Å. The crystals having $c = 230.89$ Å (form I) almost invariably undergo transformation during the course of data collection, whereas those of $c = 244.80$ Å (form II) do not. The asymmetric unit of the crystal is compatible with one monomer (Matthew's coefficient 2.66 Å^3 per dalton and 2.82 Å^3 per dalton respectively, assuming a molecular weight of 34 kDa per monomer). Both the crystal forms have the same external morphology. The data were collected at 23 ± 2°C on an MAR image plate attached to a Rigaku RU-200 rotating anode X-ray generator. The data were processed using the Denzo and Scalepack[8] suite of programs. The molecular orientation and position in the two structures, which are similar to those of wild type TS, were determined using the Molecular Replacement program AMoRE[9] and refined using X-PLOR[10]. The electron density map of form I was transformed to a grid system identical to that used for form II such that the two-fold axis relating the monomers in the two structures was superimposed. The electron density maps were examined using the program O (ref. 11).

Results

During the course of data collection, crystals of form I undergo transformation in a manner depicted in Figure 1. However, one of the eight crystals examined did not undergo transformation. It was possible to collect data to 3.1 Å resolution covering 70% of all possible reflections for the untransformed crystal. It was also possible to collect data on transformed crystals as the length of the unit cell edges remained constant within experimental errors after the transformation. Data collection and refinement statistics of forms I and II are shown in Tables 1 and 2 respectively. The agreement between the data collected on form I crystals that did not transform and the data before and after transformation for the crystal that underwent the transition between $c = 230$ Å and 244 Å is shown in Table 3. Minor variations in the pH or ionic strength might be the cause of the occasional absence of radiation-induced cell transformation of the crystals.

TS exists as a dimer in solution. The two-fold axis relating the two monomers of the dimeric protein coincides with the 2-fold crystal in both the crystal forms I and II. The structure of the dimer is nearly identical in the two forms. On application of the symmetry operators corresponding to the space group $P6_122$, four dimers were found to be in contact with the native dimer. The packing of the symmetry-related dimers in form I is shown in Figure 2. Superimposed dimers of forms I and II along with their symmetry-related dimers are depicted in Figure 3. The orientation of the nearest dimers (B, C, D, E) with respect to the reference dimer (A) in forms I and II is clearly different. A comparison of the number of the symmetry-related contacts at the interface between neighbouring dimers of both forms is shown in Figures 4 and 5. It is clear that the regions involved in contact are the same in forms I and II. Also the number of contacts are not very different. This observation suggests that the inter-dimeric contacts are similar (quasi-equivalent[12]), despite significant change in the orientation of the nearest dimer and crystal *c* parameter. In the case of form I, however, two symme-

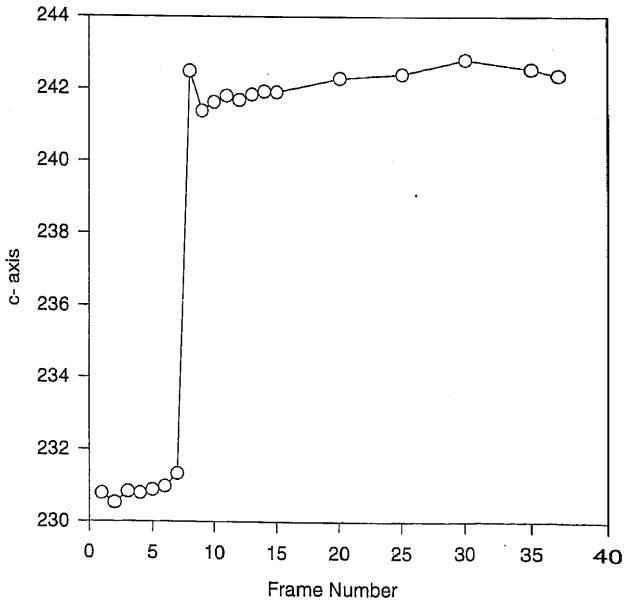

Figure 1. Plot of the *c* cell dimension as a function of exposure. Each frame was taken at a crystal to film distance of 228 mm and an exposure time of 1000 s.

try-related aspartates at position 287 originating from dimers related by 6_2 symmetry (B and D) make contact, a feature absent in form II (Figures 3 and 4). The close proximity of the aspartates of dimers (B) and (D) suggests that they are probably stabilized by hydrogen bond interactions (Figure 4), although the resolution of the structures is not sufficient to establish the details of this bonding pattern.

The following description of the crystal packing provides insights into the crystal structure transformation. The crystal 6_1 axis runs from right to left of Figure 3. Chains of closely associated dimers line up in a zig-zag pattern along the two-fold screw axes perpendicular to the crystal c axis. The separation between the nearest two-fold screw axes (skew lines separated by $c/6$) determines the c length. In Figure 3, the left-side subunit of dimer A and right-side subunits of dimers B and C are related by one of the 2_1 axes. Similarly, the right-side subunit of dimer A and left-side subunits of dimers D and E are along the second 2_1 axis. The screw axis is perpendicular to the 6_1 axis and runs vertically from the top to the bottom of the figure. The first screw axis runs from above the plane of Figure 3, at the lower corner of the left-hand side to below the plane of the paper. The second screw axis runs from below the plane of the paper at the bottom of the right-hand side to above the plane of the paper towards the top. These two screw axes are related by a crystal two-fold axis in the plane of the figure approximately at the center of Figure 3. The screw axes are also related by the crystal 6_1 axis. The zig-zag rows of molecules parallel to the screw axes therefore appear to be organized in two layers, an arrangement separated along the larger cell dimension c. The distance between the molecular chains is controlled by the hydrogen bonding interactions of Asp-287 (as shown in Figure 3) and undergoes maximum change upon disruption of the interaction between the two aspartate residues. This leads to expansion in the c-direction.

In order to understand how this cell expansion could take place without damage to crystallinity, zones which make contacts between the symmetry-related dimers in the two crystal forms were critically examined. The contacting zones and the associated residues are the same in the two crystal forms (Figure 5). The regions of the molecule involved in the contact are inherently flexible and therefore probably adapt to changes in cell parameters. To facilitate comparison of the structures and the degree of disorder in these regions of the

Table 1. Summary of crystal parameters and data statistics for the two crystal forms

	Form I	Form II
Cell parameters	$a = b = 79.3$ Å $c = 230.89$ Å	$a = b = 79.18$ Å $c = 244.8$ Å
Total number of reflections	14424	32492
Average number of times each intensity was estimated	2.43	4.05
Total number of unique reflections	6945	8024
Number of unique reflections in the resolution range 10–3.0 Å with $I/\sigma(I) > 2.0$	3924	4112
Completeness in the resolution range 10–3.0 Å with $I/\sigma(I) > 2.0$	64.1%	81.9%
Completeness in the last resolution shell 3.14–3.0 Å	60.53%	61.26%
R-merge*	11.9%	9.1%

*$R_{merge} = \Sigma \mid F_o - kF_c \mid / \Sigma F_o \times 100$.

Table 2. Refinement statistics for the two crystal forms

	Form I	Form II
Initial R^a-factor for the 4 TMS model in the cells of form A/form B	27.0%	29.9%
Initial free $R^{a,b}$-factor for the 4 TMS model in the cells of form A/form B	31.4%	31.4%
Final R^a-factor for reflections with $I/\sigma(I) > 2.0$ in the resolution range 10.0–3.0 Å	23.3%	22.2%
Final free $R^{a,b}$-factor for reflections with $I/\sigma(I) > 2.0$ in the resolution range 10.0–3.0 Å	27.1%	26.7%
Number of non-hydrogen atoms in the model	2587	2587
RMS deviation in bond angles (degrees)	2.7	2.0
RMS deviation in bond lengths (Å)	0.013	0.010

[a] R-factor $= \Sigma \mid - \langle I_h \rangle \mid \Sigma \langle I \rangle \times 100$, where I_h is the intensity of a measurement and $\langle I \rangle$ is the average of the measurements for reflection h. 4 TMS is the PDB[13] code for wtTS[9].
[b] Free R: 5% of the total number of unique reflections. This test set was not included during the course of the refinement.

Table 3. Comparison of the data-sets collected for forms I and II

Crystal form	II	I	AT : 1–7	AT : 1–54
II	–	40.9%	40.98%	12.23%
	(4112)	(3924)	(2083)	(3812)
I	30.83%	–	17.35%	40.7%
AT : 1–7	28.11%	88.5%	–	40.4%
AT : 11–54	95.32%	28.74%	29.2%	–

[a] Form I: $c = 230.8$ Å.
Form II: $c = 244.8$ Å.
Form AT : 1–7: Form I before transformation (frames 1–7 during data collection).
Form AT : 11–54: Form I after transformation (frames 11–54).
[b] Top triangular half of the matrix presents R-factors[c] and the bottom half correlation coefficients[d]. Figures in parentheses are the number of unique reflections.
[c] R-factor $= \Sigma \mid F_1 - F_2 \mid * 100 / \Sigma (F_1 + F_2)$.
[d] Correlation coefficient
$= \Sigma (F_1 - \langle F_1 \rangle)(F_2 - \langle F_2 \rangle) / \sqrt{\Sigma (F_1 - \langle F_1 \rangle)^2 \Sigma (F_2 - \langle F_2 \rangle)^2}$.

polypeptide, the maps corresponding to the two forms were sampled on identical grids. The polypeptide chains corresponding to the contacting zones were displayed and the fit of the two structures to the maps was carefully examined. This allowed an assessment of the significance of structural changes in the contacting zone that accompanies crystal transformation. No significant structural changes were discernible in the ordered regions of the molecule. As illustrated in Figure 6, the magnitude of deviations between the Cα atoms in these structures is well within the experimental errors. Thus there is no major structural change which accompanies cell transformation.

Discussion

The crystal structure of the complex of *L. casei* thymidylate synthase with dUMP and phosphate-bound forms[4] has been solved to 2.36 Å resolution. Finer-Moore *et al.*[4] have noted the presence of two crystal forms (similar to form I and form II reported in this paper), one of which undergoes transformation. This phenomenon has been reported to be reversible, albeit rarely. pH-dependent interactions have been proposed to be a probable cause; the form which undergoes transformation was crystallized at a higher pH in the study of Finer-Moore *et al.*[4]. Our observations suggest, however, that these two forms

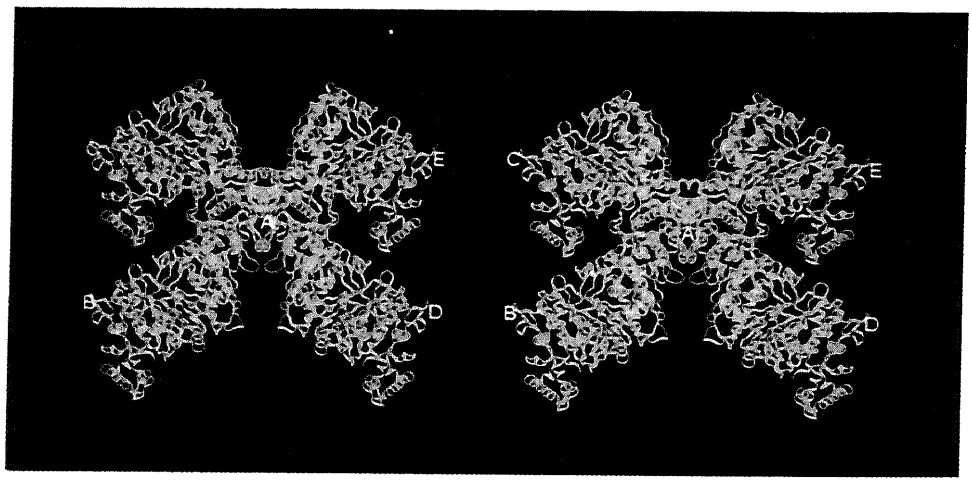

Figure 2. Symmetry-related dimers of TS in the space group $P6_122$. Each TS dimer makes contact with four neighbouring TS dimers.

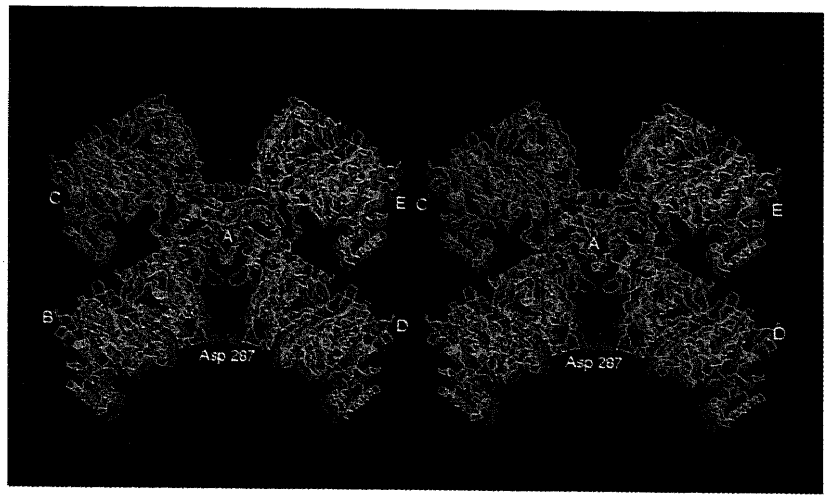

Figure 3. Superimposed dimers of forms I (green trace) and II (yellow trace) along with their symmetry-related neighbours. Also shown is the contact made by dimers B and D of form I involving aspartate 287.

could be obtained from the same crystallization well, i.e. under the same macroscopic conditions and so far we have failed to observe the reverse transformation.

The dimeric interactions of TS, which are important for its activity, remain the same in forms I and II. Thus changes which occur upon transformation are due to changes in the spatial relationship between dimers. The most likely explanation for this is an alteration in the ionization state of the aspartate residue at position 287 resulting in a change in hydrogen bonding ability and leading to the transformation from form I to II. Form I and form II structures were compared by superposing the dimers labelled A in Figures 2 and 3. The movement of the dimer labelled B was estimated by measuring the distance between the centroids calculated in the two crystal forms. A separation of 3.24 Å was obtained between the centroids of the B dimers in the two crystal forms. Examination of these two structures along with three others reported in the literature with c cell parameters of 230.2 Å[4], 240.2 Å[4] and 243.8 Å[3] leads to the conclusion that the transformation occurs due to a rotational movement of the nearest dimer about a putative pivot in the inter-dimer contact region. The rotation leads to movements of the order of ~ 5 Å at the outer edge of the neighbouring dimer in structure A when compared to structure B as shown in Figure 3. However, as the rotation is about a pivot axis close to the contact zone, no large changes in inter-dimer interactions occur. The change in the unit cell volume upon transformation probably gets compensated by the rearrangement of water molecules and possibly by the inclusion of additional molecules from the solution surrounding the crystals. This seems a plausible reason, as the crystals of TS are obtained by reducing the ionic strength of the crystallization buffer and are found to be more stable when the buffer is replaced by Milli-Q water. Thus the environment around the crucial Asp-287 may be controlled by bridging water molecules in addition to pH effects. The resolution of the X-ray data, however, does not permit investigation of the water structure in the two crystal forms.

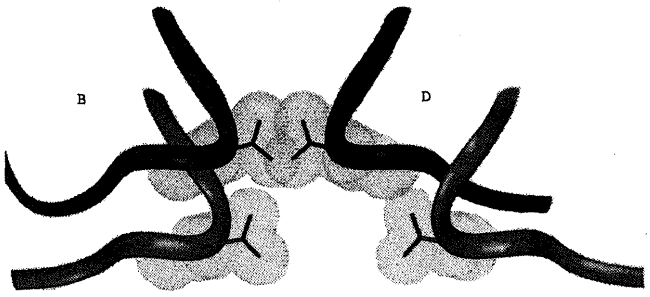

Figure 4. The intermolecular contact region around Asp-287. Shown in the dark tube is form I and that by the light tube is form II.

Transformation of crystal cell parameters upon radiation is not uncommon. That these changes could be definitively rationalized in terms of rearrangements in molecular interactions even at 3 Å resolution is surprising. This is almost certainly related to special features of the arrangement of the secondary structural elements and loop regions in TS dimer which lead to the characteristic plasticity of the TS molecule. This special aspect of TS structure has been observed earlier[4]. The molecular structure of TS in various crystal forms exhibits

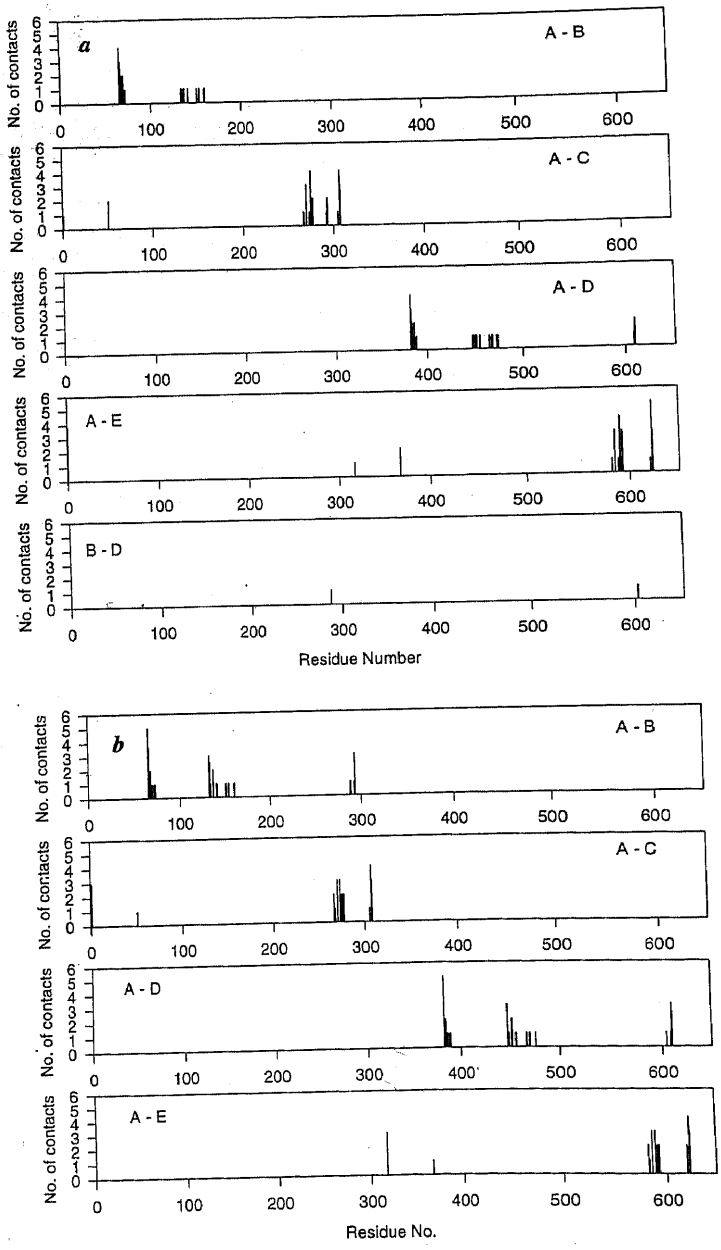

Figure 5. The number of contacts as a function of residue number is depicted for forms I and II in panels (*a*) and (*b*) respectively. The zones making intermolecular contacts appear to be intact in the two forms. The only conspicuous difference between forms I and II is the contact made by Asp-287.

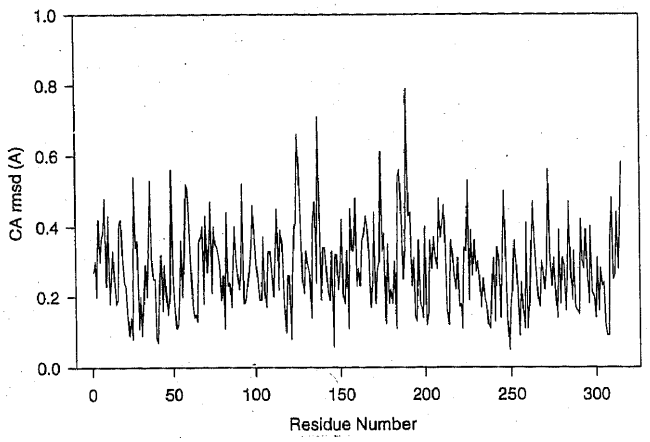

Figure 6. Magnitude of the deviations of the Cα atoms for the structures obtained in the forms I and II.

variations distributed throughout the structure. Thus any strain on the TS dimer tends to produce a number of muted changes rather than large alterations at a single site or total loss of structure. This allows the inter-dimer contact to undergo small changes in different crystal structures leading to a range of values for the crystal *c* axis lengths.

The loss of crystallinity in proteins upon prolonged exposure to X-rays is a relatively common feature. The present observation of a transformation from one crystal form to another during the process of exposure to X-rays is relatively rare. The analysis presented here of the crystalline transformation in *L. casei* TS suggests that plasticity of intermolecular contacts may play a role in such phenomena. Although Asp-287 is the only residue which appears to show significant positional changes in the two crystal forms, extensive changes in water structure cannot be ruled out at the present resolution of our structure determination.

1. Matthews, B. W., *Adv. Protein Chem.*, 1995, **46**, 249–277.
2. Carreras, M. and Santi, D. V., *Annu. Rev. Biochem.*, 1995, **64**, 721–762.
3. Hardy, L. W., Finer-Moore, J. S., Montfort, W. R., Jones, M. O., Santi, D. V. and Stroud, R. M., *Science*, 1987, **235**, 448–455.
4. Finer-Moore, J., Fauman, E. B., Foster, P. C., Perry, K. M., Santi, D. V. and Stroud, R. M., *J. Mol. Biol.*, 1993, **232**, 1101–1116.
5. Gokhale, R. S., Agarwalla, S., Francis, V. S., Santi, D. V. and Balaram, P., *J. Mol. Biol.*, 1994, **235**, 89–93.
6. Prasanna, V., Ph D thesis, Indian Institute of Science, 1998.
7. Gonzalez, A. and Nave, C., *Acta Crystallogr.*, 1994, **D50**, 874–877.
8. Otwinowski Z. , Proceedings of the CCP4 study weekend: 'Data Collection and Processing', 29–30 January 1993, Compiled by: Sawer, L., Issacs, N. and Bailey, S., SERC Daresbury Laboratory, England, pp. 56–62.
9. Navaza, J., *Acta Crystallogr.*, 1994, **A50**, 157–163.
10. Brunger, A. T., X-Plor, Version 3.1, A system for X-Ray Crystallography and NMR, New Haven CT, Yale University Press, 1992.
11. Jones, T. A., Zou, J-Y., Cowan, S. W. and Keildgaard, M., *Acta Crystallogr.*, 1991, **A47**, 110–119.
12. Caspar D. L. D. and Klug A., in *Cold Spring Harb. Symp. Quantita. Biol.*, 1962, **XXVII**, 1–24.
13. Bernstein, F. C., Koettizde, T. F., Williams, G. J. B., Meyer, E. F. Jr., Brice, M. D., Rodgers, J. R., Kennard, O., Shimanouchuli, T. and Tasumi, M., *J. Mol. Biol.*, 1977, **112**, 535–542.

ACKNOWLEDGEMENT. We thank CSIR, India for financial support.

Received 27 April 1998; revised accepted 2 July 1998